JOURNAL OF APPLIED ELECTROCHEMISTRY **28** (1998) 955–962

Characterization of PTFE-bonded porous carbon electrodes tested in a 100 W phosphoric acid fuel cell (PAFC) stack using XPS and ICP–AES techniques

M. GHOUSE

Energy Research Institute, King Abdulaziz City for Science and Technology (KACST), PO Box 6086, Riyadh 11442, Kingdom of Saudi Arabia

Received 8 June 1997; revised 7 January 1998

A 100 W PAFC stack with 12 cells was assembled using in-house developed PTFE-bonded gas diffusion porous carbon electrodes, graphite bipolar plates and aluminium external gas manifolds. The stack was operated for 1000 h continuously with acid management, using H_2 and air at 1 bar and at 175 °C. After completion of the test the stack was disassembled and the electrodes were characterized using X-ray photoelectron spectroscopy (XPS) and inductively coupled plasma–atomic emission spectroscopy (ICP–AES) techniques. The XPS and ICP–AES results revealed the presence of platinum in the electrolyte matrix layers (SiC + PTFE) and carbon mat layers (carbon + PTFE), which were applied on the cathodes and the anodes, respectively. This clearly indicates that there was a migration of platinum from cathodes to anodes during the stack operation. This may have occurred when operating the stack at it's open circuit voltage (OCV) while taking measurements of stack voltage and current for the I/V curves.

Keywords: *phosphoric acid fuel cell*, *PTFE-bonded gas diffusion porous carbon electrodes*, *platinum migration*, *carbon mat layer*, *matrix layer*, *catalyst layer*

1. Introduction

The most important factor for performance improvement of gas diffusion porous carbon electrodes in phosphoric acid fuel cells (PAFC) is the optimum physical structure of the catalytic layer as the electrochemical reaction occurs at the three phase junction of solid electrode, liquid and gas [1]. It is known that even when the same percentage of materials, such as Pt/C catalyst powder and PTFE, are prepared to the same ratios, the characteristics of the electrode may not be the same because they depend on the physical structure, porosity, pore volume, microstructure, platinum content, platinum crystallite size and PTFE content. The preparation of gas diffusion porous carbon electrodes is as much an art as a science. Although extensive R&D has been done on PAFC technology during the last 25 years, catalysts are still not completely stable under some operational conditions. For example, platinum crystallites grow with time under severe conditions such as in hot H_3PO_4 at 190 °C. It is suggested that there are two mechanisms involved: platinum dissolution/redeposition [2, 3] and platinum migration from cathode to anode [4, 5]. Connolly *et al.* [2] reported that a local cell may be formed between larger platinum and smaller platinum crystallites, where platinum ions are transported from smaller particles to larger ones. Tseung and Dhara [3] concluded that the platinum sintering occurs by a dissolution/redeposition cycle, where small particles dissolve in solution by virtue of their greater surface energy and diffuse along a concentration gradient to the larger particles. Blurton *et al.* [4] demonstrated that crystallite migration was the mechanism of particle growth based on the lack of potential dependence on surface area loss, and the tailing on the large diameter side of particle size distribution of supported platinum catalyst. Gruver *et al.* [5] found that platinum crystallite migration-coalescence was a major mode of platinum surface loss. Several authors [3, 6, 7] reported that the sintering process occurred due to the surface diffusion of platinum atoms to sites of lower surface energy. Bett *et al.* [7] studied the effect of support, potential dependence, platinum loading dependence and environment on sintering. Hyde *et al.* [8] reported reduction of platinum in a cathode during cell operation and concluded that platinum had migrated from cathode to anode. In the present investigation, an attempt has been made to use XPS and ICP–AES techniques to characterize the porous carbon electrodes tested in the 100 W PAFC stack.

2. Experimental details

2.1. *Assembly of the 100 W PAFC stack*

A 100 W PAFC stack (no. 100-05) was assembled using in-house developed components, including carbon mat layers, anodes, cathodes, electrolyte

0021-891X © 1998 Chapman & Hall

matrix layers, graphite bipolar plates and external gas manifolds. The details of the fabrication of the porous carbon electrodes and graphite bipolar plates have been described by Ghouse *et al.* [9–11]. The electrodes were 20 cm × 12 cm × 0.6 mm including a carbon support of 0.35 mm; the graphite bipolar plates were 20 cm × 12 cm × 6.4 mm including an impervious layer at their centres [11]. Carbon mat layers with 15 wt % PTFE powder and 85 wt % carbon was applied over the anodes, and matrix layers containing 94 wt % SiC and 6 wt % PTFE were applied over the cathodes. The electrodes were edge sealed with PTFE tape to give an effective area of 125 cm^2 , and for 24 h before assembly they absorbed 99% H_3PO_4. The stack had 12 cells connected in series with a load of 12 incandescent bulbs connected in parallel. Each bulb was rated at 10.8 W which gave a total d.c. generating power of 130 W. The stack was operated continuously for 1000 h at a temperature of 175 °C. Commercial H_2 with 15 vol % CO_2 was used as the fuel, air was used as an oxidant, and acid management was employed. A constant load was maintained such that the d.c. output was 22 A at a stack voltage of 6 V. A cross section of mono cell 6 as assembled in the 100 W PAFC stack is shown in Fig. 1. Electrodes from cells 6 and 7 were used for the characterization studies. They were first washed with hot water to remove the phosphoric acid and then characterised using XPS and ICP–AES techniques to study the platinum migration from cathode to anode during the stack operation.

2.2. *X-ray photoelectron spectroscopy (XPS)*

The XPS spectrum of cell 6 was generated using K_α radiation from a Mg anode operated at 14 kV and 23 mA, and with the vacuum system base pressure set to 2×10^{-8} torr for the duration of the data collection. The samples containing the silicon carbide, taken from the cathode matrix layer, charged up a little but did not cause noticeable distortion of the spectra. This technique has been employed by several authors to characterize the electrocatalyst surface [12] and fuel cell electrode surfaces [13–18], both before and after conducting their long term tests to study their surface properties.

2.3. *Inductively coupled plasma–atomic emission spectroscopy (ICP–AES)*

Inductively coupled plasma–atomic emission spectroscopy (ICP–AES) uses an argon plasma formed by the interaction of an r.f. field with an ionised argon gas stream. This spatially stable, chemically inert plasma produces an ideal environment for optical emission spectroscopy. The argon carrier gas aspirates the liquid sample into the spray chamber and transports the smaller sample droplets into the plasma. The high temperature in the plasma dissociates the sample material into atoms and ions which are excited to electronic states above the ground state. The characteristic emission of visible and ultraviolet light by the excited species on their return to the ground state represents the basis for optical emission spectroscopy. The spectrometer sorts the various wavelengths and measures the intensity of the spectral lines which are specific to individual elements being analysed. Photomultiplier tubes measure the intensities by converting the emitted light into an electrical signal proportional to the concentration of the analyte producing the emission. The carbon mat layer and anode catalyst layer from cells 6 and 7 were prepared as samples by cutting them into small pieces and weighing them to the nearest 0.0001 g. The test

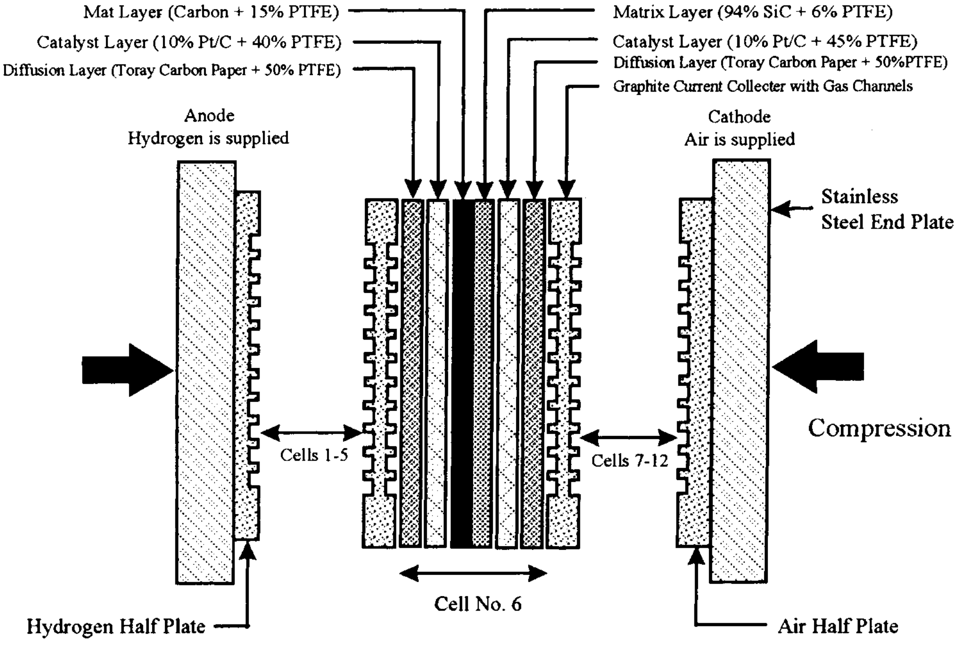

Fig. 1. Schematic diagram of mono cell 6 in the 100 W PAFC stack (12 cells).

samples were then separately digested in aquaregia at slow heating reflux for 30 min. However, since the aquaregia at this point did not dissolve the material due to the high content of carbon and PTFE. The samples were slowly dried and ashed at 500 °C overnight. The samples were then cooled to room temperature and digested with 10 ml of aquaregia. After cooling, the dissolved materials were diluted to 50 ml with deionised water and analysed by ARL ICP–AES (model 3580B). A scan run was carried out to check for other elements. The concentration of these elements in each sample was then determined. The error in the values determined by this technique is 3%.

3. Results and discussion

3.1. *100 W PAFC stack*

Figures 2 and 3 show stack voltage vs stack current and average cell voltage vs current density, respectively. It can be seen from the Fig. 3 that the current density obtained was about 175 mA cm^{-2} at an average cell voltage of 0.52 V. This was achieved with an operating temperature of 175 °C with H_2 and air at 1 bar. Figure 4, a plot of stack power and resistance against operating time, shows that there was a decrease in power of about 3 W and an increase in resistance from 23–25 mΩ over the testing period of 1000 h.

3.2. *X-ray photoelectron spectroscopy (XPS)*

Table 1 shows the summary of the XPS analysis of the electrodes before and after testing them in the 100 W PAFC stack. It depicts the binding energy values relevant to six samples with values presented with units of eV. C1s binding energy at 284.6 eV is taken as reference for the correction of charging the chemical origin of most species for the various samples.

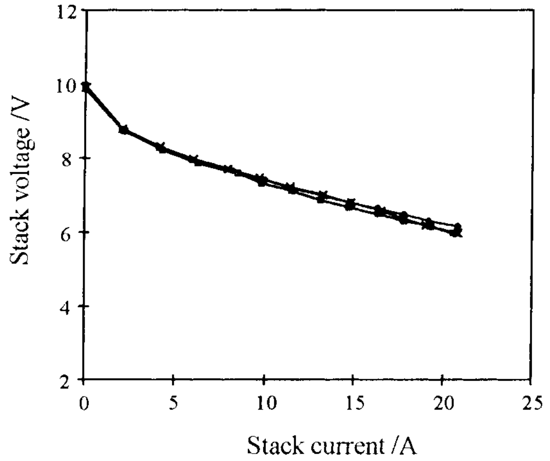

Fig. 2. Stack voltage against stack current operating conditions. Fuel: H_2, 180 l h^{-1}, 1 bar; oxidant: air, 400 l h^{-1}, 1 bar; temperature: 175 °C, electrode area: 125 cm^2, H_3PO_4: 99%; with acid management (■) 100 h, (●) 500 h, (×) 1000 h.

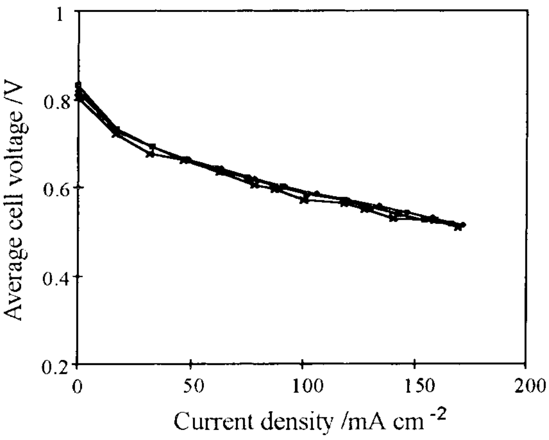

Fig. 3. Average cell voltage against current density, operating conditions are same as in Fig. 2. (■) 100 h, (●) 500 h, (×) 1000 h.

Figure 5(a) to (f) shows the XPS general scan spectra before and after testing them in the 100 W stack for a period of 1000 h. Figure 5(a) and (b) shows the anode carbon mat layers, Fig. 5(c) and (d) shows the anode catalyst layers, and Fig. 5(e) and (f) shows the cathode matrix layers. The Figures show bonding energy against *N*(*E*)/*E*, where *N*(*E*) is the number of photoelectrons and *E* is the energy interval. From Fig. 5(a) and (b) the major peaks identified in the spectra are: F1s, C1s (carbide, fluorine, and graphite), O1s, F(KLL), O(KLL), Si 2p, Si 2s, P2p and Pt 4f. The F signals result from the surface exposed PTFE in both anodes and cathodes and may indicate the relative amount of this material at the electrode surface. The carbon in the mat layer is due to its composition of 85% C with 15% PTFE. The carbide peaks are due to the matrix layer containing 94% SiC with 6% PTFE. The two carbon peaks at 285 eV and 292 eV are due to graphite and carbon, respectively. These are due to the 54% carbon powder in the catalyst powder and carbon in the form of the fluorocarbon component of the 40% PTFE which was added as a binder in order to

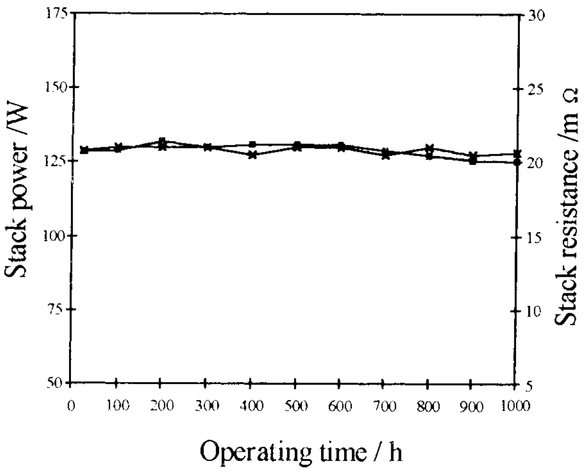

Fig. 4. Stack power and stack resistance against operating time, operating conditions are same as in Fig. 2, (■) Stack power and (×) stack resistance.

Table 1. Summary of the XPS analysis reports of the anodes, cathodes, carbon mat and matrix layers, before and after their continuous test for 1000 h in a 100 W PAFC stack

Sample	*C1s Carbide*	*C1s Graphite*	*C1s Fluoro*	*O1s Oxygen*	*Si2p Carbide*	*Si2p Oxide*	*P2p Phosphorus*	*Pt 4f Platinum*	*F1s Fluorine*
ABT-T-CM	–	refer	–	532	–	–	–	–	688.9
AS6-T-CM	–	refer	291.8	532.6	100.5	103.7	133.8	71.2	688.9
ABT-B-CAT	–	refer	292	Broad	–	–	134	71.3	689
AS6-B-CAT	–	refer	532	532	–	–	–	71.4	689
CBT	282.4	refer	291.5	532	100.4	103.4	–	–	689.5
CS6	282.3	refer	291.7	533	100.2	103.9	134	71.2	688.8

ABT-T-CM: anode–carbon mat layer-before test, AS6-T-CM: anode–carbon mat layer-after test.
ABT-B-CAT: anode–catalyst layer-before test, AS6-B-CAT-: anode–catalyst layer-after test.
CBT: cathode-matrix layer before test, CS6: cathode-matrix layer after test (these are top layers).
(B- refers to 'bottom' and T- refers to 'top').

achieve the optimum electrode hydrophobicity. The platinum is the result of the catalyst at the surface of the anode (as prepared) before test. The presence of platinum in the carbon mat and matrix layers after the test may be due to migration from the cathode. The intensity of the carbon peak in the tested carbon

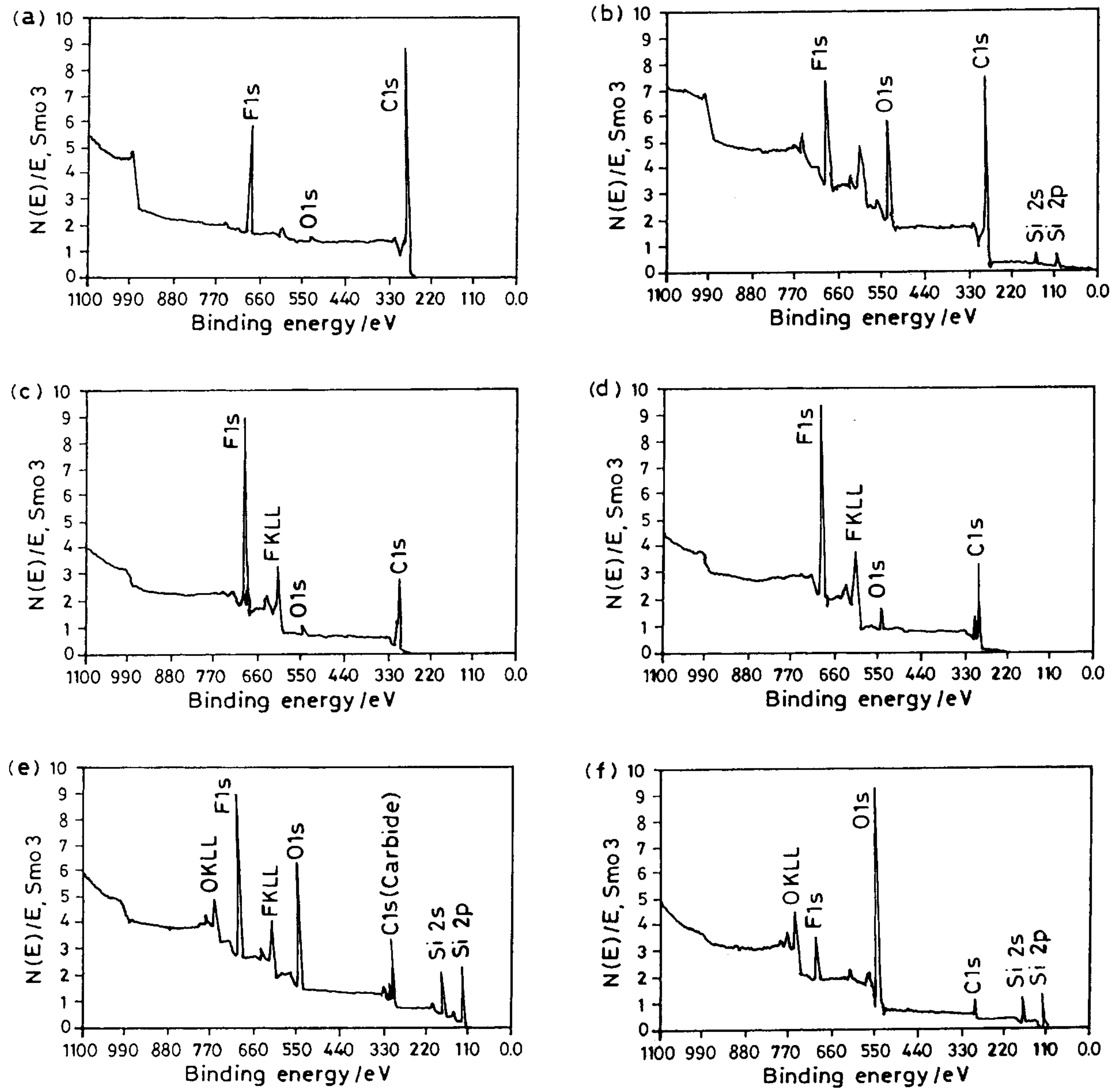

Fig. 5. XPS general scan spectra of: (a) ABT-T-CM (anode mat layer before test), (b) AS6-T-CM (anode mat layer after test), (c) ABT-B-CAT (anode catalyst layer before test), (d) AS6-B-CAT (anode catalyst layer after test), (e) CBT (cathode matrix layer before test), (f) CS6 (cathode matrix layer after test).

mat layer was lower, which may be due to carbon corrosion as the carbon layer was at the top of the anode-reaction side, that is, above the anode catalyst layer, which was in direct contact with hot phosphoric acid at 175 °C. Other authors have reported similar behaviour elsewhere [19]. A small amount of silicon was observed on the carbon mat layer; this occurred during the separation of the anodes and cathodes with matrix layer containing SiC and PTFE from the test cell assembly. The removal involved a peeling motion which caused a separation of the carbon mat layer and the matrix layer. The oxygen at the surface of the cathode before testing is atmospheric oxygen, and the large amount after testing is from the air supplied to the cathode while the stack was being operated (Fig. 5(e) and (f)).

From Fig. 5(a) and (b), it can be seen that the oxygen peak increased after testing the anode, with the largest increase in the mat layer. This clearly indicates that there was a crossover of air to the anode side, causing a decrease in stack voltage and an increase in stack temperature. The increase in stack temperature would cause depletion of the acid in the matrix. Therefore optimum pore volume and pore diameter of the electrodes should be used. Also it is seen that there was no major change in the F and C peaks of the anode catalyst as it was below the carbon mat layer. Figure 5(e) and (f) shows a reduction in carbide (SiC) in the cathode matrix layer after testing. This may have been caused by the formation SiO_2 by reaction with the hot phosphoric acid in the presence of air. Figure 5(e) and (f) shows a decrease in the intensity of the F1s peak of the tested cathode matrix layer relative to the intensity of the same peak obtained in the earlier XPS analysis. This clearly indicates a loss of PTFE content from the cathode surface after testing in the stack. This may be due to corrosion of the PTFE in the matrix.

Figure 6(a) and (b) shows the XPS spectrum of the Pt 4f region of the anode catalyst layer before and after testing, and Fig. 6(c) and (d) shows the XPS spectrum of the Pt 4f region of the tested anode mat layer and the tested cathode matrix layer. Platinum peaks can be seen on the cathode electrolyte matrix layer and the anode carbon mat layer. Before testing there was no platinum on the carbon mat layer and cathode matrix layer, but after testing in the stack, platinum peaks were found. The Pt 4f XPS spectra show one doublet peak for which the binding energies were 71.2 eV and 75.5 eV, respectively. It appears from Fig. 6(c) and (d) that small platinum particles migrated from the cathode, through the cathode matrix and the anode carbon mat layer, to the anode. This observation is similar to that reported elsewhere [20, 21].

Table 2 shows the atomic concentration of the anode carbon mat layer before and after testing in the stack. The concentration of oxygen is due to the environment, while carbon and fluorine are from carbon powder and PTFE, respectively. It is seen that the concentration of oxygen is high in the tested mat layers. It is also seen that there is a drastic reduction of carbon in the mat layer. This might be due to carbon corrosion as reported elsewhere [14–18]. It is

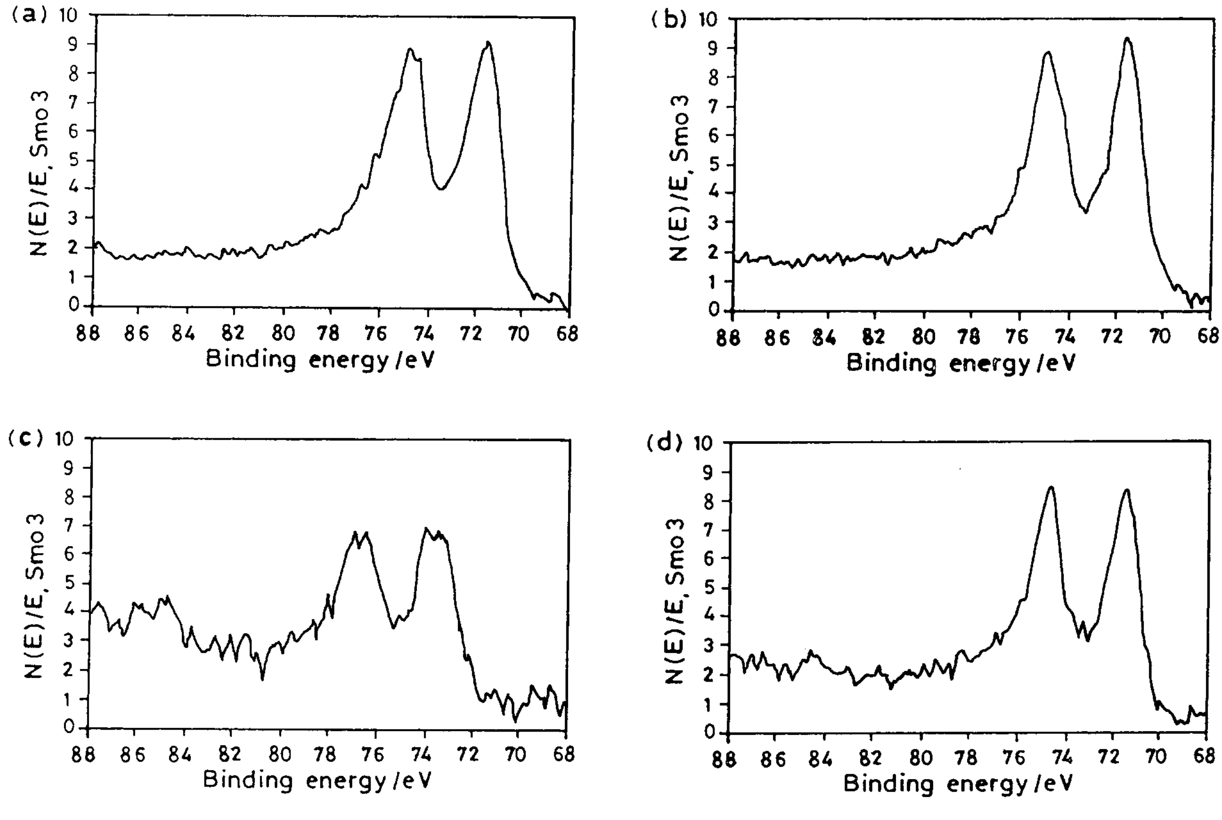

Fig. 6. XPS spectra of Pt 4f region of: (a) ABT-B-CAT (anode catalyst layer before test), (b) AS6-B-CAT (anode catalyst layer after test), (c) AS6-T-CM (anode mat layer after test), (d) CS6 (cathode matrix layer after test).

Table 2. Atomic concentrations of the carbon mat (CM) layers (applied on the anodes)

Elements analysed	*After testing: AS6-T-CM*		*Before testing: ABT-T-CM*	
	Concentration/%	*Sens. factor*	*Concentration/%*	*Sens. factor*
Si2p	3.84	0.270	–	–
P2p	0.44	0.390	–	–
O1s	15.27	0.660	1.24	0.665
C1s	64.72	0.25	83.1	0.27
F1s	15.65	1.000	15.7	1.000
Pt 4f	0.08	4.400	–	–

also important to note that the increase in the concentration of oxygen is due to crossover of air from the cathode. Platinum was not present in the as-prepared carbon mat layer, but was found in the tested carbon mat layers. The platinum migrated from the cathodes to the anodes through the matrix and carbon mat layers. This is in agreement with what other authors have reported [20–23].

Table 3 shows the atomic concentration of various elements, including O, C, F and Pt in the anode catalyst layers before and after testing. It is observed that the fluorine concentration is slightly reduced in the tested anode from the stack. It is evident that platinum particles are migrating from the cathode to the anode during the operation of the stack and are being deposited over the anode. Therefore, the platinum content in the tested anodes is more than that in the as-prepared anode, as shown in Table 3. This may be one of the reasons why higher platinum loadings of 25 wt % are commonly used in PAFC stack and power plant cathodes; it would tend to lengthen their operational life.

Table 4 shows the atomic concentration of the cathode matrix layer before and after testing. It is seen that platinum was not found in the as-prepared matrix layer containing SiC + PTFE. However, there was a slight platinum content in the tested matrix layer. This observation is similar to that reported elsewhere [8, 22]. Ross [20] estimated platinum flux transport of dissolved platinum ion in two cases of platinum migration. The first was a migration of platinum from cathode to anode, and the second was a migration from small particles to large ones, which can be interpreted as an analogy to the Ostwald ripening model. It is seen from Table 4 that the concentration of oxygen is low in the case of the matrix layer before testing, which may be due to the environment. On the other hand, the oxygen concentration is very high in the case of tested matrix layers as air was supplied to the cathode during stack operation. The reasons for the migration of the platinum may be explained as suggested by other authors [8, 20, 22, 23].

3.3. *Inductively coupled plasma–atomic emission spectroscopy (ICP–AES)*

Table 5 shows the ICP–AES analysis of the anode carbon mat and catalyst layers after testing in the stack (Fig. 1). This shows a migration of platinum from the cathode to the anode. The platinum in the anodes increased from an initial value of 6 wt % to

Table 3. Atomic concentrations of the catalyst (CAT) layers–anode

Elements analysed	*After testing: AS6-B-CAT*		*Before testing: ABT-B-CAT*	
	Concentration/%	*Sens. factor*	*Concentration/%*	*Sens. factor*
F1s	34.98	1.00	37.06	1.00
P2p	0.31	0.390	–	–
O1s	4.01	0.660	2.54	0.66
C1s	60.50	0.25	60.21	0.25
Pt 4f	0.20	4.400	0.18	4.40

Table 4. Atomic concentration of the matrix layers–cathode

Elements analysed	*After testing: CS6*		*Before testing: CBT*	
	Concentration/%	*Sens. factor*	*Concentration/%*	*Sens. factor*
Si2p	24.68	0.270	23.19	0.27
P2p	0.60	0.390	–	–
O1s	49.69	0.660	18.62	0.66
C1s	16.93	0.25	34.71	0.25
F1s	8.05	1.000	23.47	1.000
Pt 4f	0.05	4.400	–	–

Table 5. Platinum content (wt %) of electrode anode catalyst and carbon mat layers after testing in the 100 W PAFC stack as determined using ICP–AES technique

Elements analysed	*Sample 101 (cell 6) Cat layer after test*	*Sample 102 (cell 6) Mat layer after test*	*Sample 103 (cell 7) Cat layer after test*	*Sample 104 (cell 7) Mat layer after test*	*Sample 105 Cat layer before test*	*Sample 106 Cat layer before test*
Ca	0.03	0.03	0.04	0.02	0.05	0.05
Cr	0.03	<0.01	0.02	<0.01	0.03	0.02
Fe	0.01	0.06	0.01	0.05	0.02	0.03
Na	<0.01	<0.01	0.02	<0.01	0.12	0.5
P	0.01	0.12	0.08	0.12	–	–
Pt	6.50	0.36	6.35	0.31	5.98*	5.99*
Sn	0.15	0.16	<0.01	<0.01	0.92	0.47
Zn	0.07	0.03	0.02	0.02	0.01	0.01

*Composition of as-prepared Anode: 6 wt % Pt, 54 wt % Carbon, 40 wt % PTFE.

between 6.35 and 6.5 wt %. It is also observed that, while the carbon mat layer was initially without platinum, it contained platinum after operating the cells in the stack for 1000 h. It is evident, therefore, that platinum is migrating from cathode to anode. These results are in agreement with those of other authors [13–17]. It is confirmed by the analysis of the tested electrodes (mat layer and matrix layer) for platinum using both XPS and ICP–AES techniques that there is a strong evidence of migration of platinum from the cathode to the anode and deposition over the anode layers. The higher platinum content in the tested anode catalyst layer, as seen in Table 3, clearly shows that there was a migration of platinum from the cathode. A possible reason for this migration was that the stack was operated at its OCV for periods of 30–40 minutes during the testing phase, as part of the voltage and current measurement for the I/V curves. Therefore, it is recommended that stacks should not be operated at their OCV for long periods. Additionally, when shutting down the stack, the load should be removed, the hydrogen gas shut off and purging with nitrogen gas should be carried out until the stack cools down to about 50 °C.

4. Conclusions

The following conclusions have been drawn:

(i) The current density obtained was approximately 175 mA cm^{-2}, at an average cell voltage of 0.52 V. Hydrogen as the fuel and air as the oxidant were supplied at 1 bar, and the operating temperature was maintained at 175 °C. 10 wt % Pt/C catalysts were used for the anodes and cathodes.

(ii) The power loss of the stack was 3 W over a testing period of 1000 h. This may have been due to a slight increase in platinum crystallite size during stack operation.

(iii) The presence of platinum in both mat layer and matrix layer was detected by both XPS and ICP–AES techniques.

(iv) A platinum content of 0.30–0.35 wt % was found in the tested anode carbon mat layer, and 6.35–6.50 wt % Pt was found in the tested anodes analysed with the ICP–AES technique. This clearly indicates platinum migration from the cathodes during the operation of the stack and deposition on the anodes.

(v) The main reason for migration of the platinum from cathode to anode during testing was the operation of the stack at its OCV during I/V measurement. Therefore, the stack should never be operated at its OCV for long periods.

Acknowledgements

The author would like to thank Eng'r Fahad S. Huraib, Solar Programs Director, and Eng'r Hassan Abaoud, Hysolar Program Manager, Energy Research Institute, King Abdulaziz City for Science and Technology (KACST), for their constant encouragement and support during this work. Also, the author's thanks are due to Drs M. H. Mohammed and K. M. A. Attar of the Research Institute, King Fahd University of Petroleum and Minerals (KFUPM), Dhahran, Kingdom of Saudi Arabia, for their cooperation during the analysis of the fuel cell electrode samples.

References

[1] S. Motoo, M. Watanable and N. Furuya, *J. Electranal. Chem.* **160** (1989) 351.
[2] J. F. Connolly, R. J. Flannery and B. L. Meyers, *J. Electrochem. Soc.* **114** (1967) 241.
[3] A. C. C. Tseung and A. C. Dhara, *Electrochim. Acta* **20** (1975) 681.
[4] K. F. Blurton, H. R. Kunz and D. R. Rutt. *ibid* **23** (1978) 183.
[5] G. A. Gruver, R. F. Pascoe and H. R. Kunz, *J. Electrochem. Soc.* **127** (1980) 1219.
[6] K. Kinoshita, K. Routsis, J. A. S. Bett and C. S. Brooks, *Electrochim. Acta* **23** (1978) 953.
[7] J. A. S. Bett, K. Kinoshita and P. Stonehart, *J. Catal.* **41** (1976) 124.
[8] P. J. Hyde, C. J. Maggiore and S. Srinivasan, *J. Electroanal. Chem.* **168** (1984) 383
[9] M. Ghouse, A. Al-Boeiz, H. Abaoud and M. Al-Garni, *Int. J. Hydrogen Energy* **20**(9) (1995) 727.
[10] A. Al-Boeiz, M. Ghouse and M. Al-Garni, Proceedings of the 16th World Energy Council Conference, Tokyo, Japan, 8–13 Oct. (1995) p. 257.

[11] M. Ghouse, A. Al-Boeiz, M. Al-Garni and H. Abaoud, *The Arabian Jo. Sci. & Eng*. **20**(4 B) (1995) 835.

[12] O. Savadogo, *J. Electrochem. Soc*. **139** (1992) 1082.

[13] V. Alderucci, V. Recupero, L. Pino, R. Di Leonardo, D. L. Cocke, N. Giordano and F. Parmigiani, *J. Appl. Electrochem*. **20** (1990) 811.

[14] O. Savadogo and A. Essalik, *J. Electrochem. Soc*. **141** (1994) L92.

[15] A. Essalik O. Savadogo and F. Ajersch, *J. Electrochem. Soc*. **142** (1995) 1368.

[16] O. Savadogo and A. Essalik, *ibid*. **143** (1996) 1814.

[17] O. Savadogo and A. Essalik Proceedings of the First International Symposium on New Materials for Fuel Cell Systems, 9–13 July (1995), Montreal. Canada, p. 688

[18] M. T. Paffett, W. Hutchinson, J. D. Farr, P. Papin, J. G. Beery, S. Gottesfeld and J. Feret, *J. Power Source* **36** (1991) 137.

[19] P. Stonehart, *Carbon* **22** (1994) 423.

[20] P. N. Ross, LBL Report no. LBL-19766-Rev (1985).

[21] E. Yearger, P. Bindra, S. Clauser and S. Sarangpani, EPRI Report no. EM-1814 (1981).

[22] J. Argane, T. Murahashi and T. Odaka, *J. Electrochem. Soc*. **135** (1988) 844.

[23] A. Pebler, *J. Electrochem. Soc*. **133** (1986) 9.